

Abstract

The common colon cancer drug CPT-11 and its active metabolite SN-38 have a dose-limiting side effect of severe diarrhea in patients. The dose-limiting side effects of CPT-11 arise when the metabolite SN-38G is reactivated in the intestines by β -glucuronidases (GUS) from bacteria. Previous work found selective inhibitors that bind to a loop region near the active site in different species and are effective in alleviating CPT-11 induced diarrhea in mice. The GUS from *Bacteroides dorei* does not have this loop. We sought to kinetically characterize the processing of SN-38G by this GUS and compare it with other GUS enzymes from common bacteria. We found that GUS from *B. dorei* was less effective than enzymes from other bacteria, however it did process SN-38G with a K_m of $21 \pm 2 \mu\text{M}$ and a k_{cat} of $5.9 \pm 0.2 \text{ s}^{-1}$. Therefore, new inhibitors may need to be designed that do not require an active site loop for have maximal chemotherapeutic effectiveness against CPT-11 induced diarrhea. We also attempted to characterize the response and growth of *Escherichia coli* in the glucuronidated forms of Diclofenac and estriol. From this, we determined that higher than $25 \mu\text{M}$ and 100 nM of substrate, respectively are necessary to maintain growth.

Introduction

The human intestinal microbiota is comprised of over 100 trillion organisms, ranging from bacteria to viruses and fungi¹. These organisms form a complex and essential symbiotic relationship within the human body. While often beneficial, they can be linked to several diseases and disease states including diabetes, atherosclerosis, obesity, malnutrition, cancer, gastrointestinal (GI) inflammatory disorders, and neurological diseases².

One bacterial enzyme, β -glucuronidase (GUS), produced by numerous species of gut bacteria, has been shown to reactivate a common chemotherapeutic for colorectal cancer, irinotecan (CPT-11), while in the intestinal lumen. CPT-11 is hydrolyzed by a carboxylesterase enzyme to form the active metabolite SN-38. It then “poisons the catalytic cycle of human topoisomerase I, which manages the super-helical tension associated with DNA metabolism and

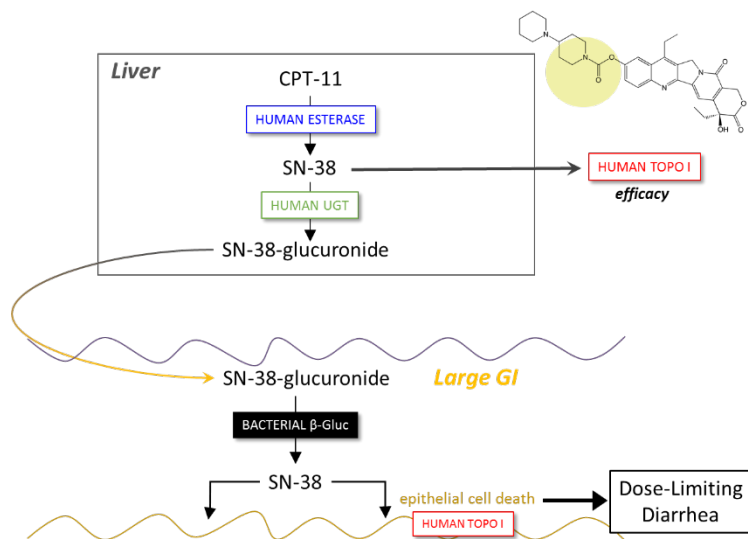


Figure 1. Mechanism of CPT-11 Toxicity Schematic

is preferentially active in rapidly dividing cells.”^{3,4} After completing its function, SN-38 is deactivated by UDP-glucuronosyl-transferases, which add a glucuronide sugar to SN-38, transforming it into the inactive form SN-38G.² It is then sent to the GI tract to be excreted.

However, once it enters the intestinal lumen, this glucuronide

moiety is cleaved off by β -glucuronidase enzymes (GUS) produced by bacterial species within the GI microbiota. The reactivated SN-38 attacks and kills the gut epithelial cells. This results in the dose-limiting side effect of severe diarrhea, noted in phase I clinical trials of the drug, and the FDA package insert for irinotecan which indicate that “up to 88% of patients experience diarrhea and 31% show grade 3–4 diarrhea” which limit efficacy of this drug.^{5,2} Finding ways to inactivate GUS is key to prevent these harmful side effects, allowing physicians to increase dosage and thereby increase efficacy of this drug.

Because of the vital functions that the GI microbiota play in maintaining health, killing bacteria within the GI tract is not an acceptable solution to reducing the amount of GUS enzyme. Inhibiting the activity of this enzyme is another option—this will selectively eliminate the GUS enzyme from reactivating SN-38, while still allowing the microbiota to survive. Through structural and chemical biology, several potent inhibitors of GUS have been identified in a high-throughput screen⁶. These inhibitors bind at “bacterial loops” at the active site of the enzyme. However, the architecture of the active site varies among different enzymes in the GUSome, resulting in different loop lengths and shapes. From the Human Microbiome Project Database, fecal samples from 139 individuals were obtained resulting in 3013 unique GUS sequences. It was found that GUS enzymes fall in to 6 general categories: Loop 1, Loop 2, Mini-Loop 1, Mini-Loop 2, Mini-Loop 1 and 2 and No Loop⁷. Of special interest are the No Loop GUS enzymes. These are the most common category of GUS, making up an average of 49% of all GUS enzymes in the microbiome⁷. Because all inhibitors thus far work by binding to a loop motif, the rate at which the No Loop GUS enzymes cleave β -glucuronides is critical to determining inhibitor efficacy in patients. *Bacteroides dorei* is a representative No Loop GUS producing species, with known crystal structures⁷ and is a good model for kinetic characterization of No Loop GUS enzymes.

The composition of an individual’s gut microbiota remains relatively stable over the course of their lives, with fluctuations arising usually because of environmental, developmental and pathological events. When an individual undergoes chemotherapy, there is an increase of glucuronidated compounds, from inactivated therapeutics, entering the intestinal lumen. Gagnière et al. note that “alterations in colonization resistance due to, e.g., pathogens or antibiotics treatment, probably increase the risk of gastrointestinal affections.”¹ Non-steroidal

anti-inflammatory drugs (NSAIDs) are another source of glucuronidated compounds in the intestinal lumen. While usually safe, long-term usage can lead to several adverse GI effects, including bleeding, protein loss and strictures⁸. In mouse studies, acyl glucuronides and phenol glucuronides of diclofenac (DCF) were found in the mouse intestines following a single dose⁹. Similar to glucuronidated chemotherapeutics, the bacterial β -glucuronidases reactivated the NSAID in the lumen, causing gut epithelial cells to be exposed to high concentrations of active NSAID, leading to cell death⁸. Inhibitors of GUS have been shown to protect mice from NSAID driven enteropathy, by preventing cleavage of the glucuronidated NSAIDs⁸. Understanding how relative bacterial abundances change in response to introduction of new glucuronidated compounds can help direct targeted therapy and use of inhibitors for maximal efficiency and protect from adverse side effects among a range of different drugs.

Methods

I. Expression and Purification of Enzymes

The full-length *B. dorei* β -glucuronidase (BdGUS) gene was purchased from Bio Basic in the pUC57 vector. The mature gene lacking the signal peptide was amplified and inserted into the pLIC-His vector. Purified protein was obtained by members of the Redinbo Lab.

II. PNPG Assay

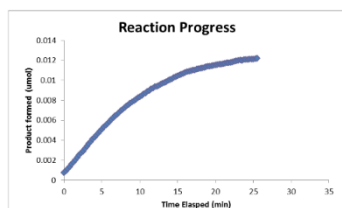
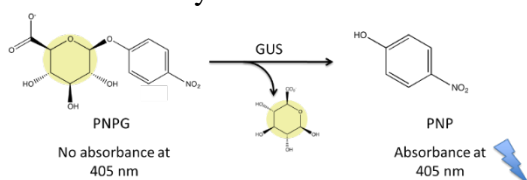


Figure 2. Schematic of PNPG Assay

Para-nitrophenyl glucuronide (PNPG) was purchased as a solid and suspended in water to a concentration of 100 mM. Reactions were conducted in triplicate in 96-well, black, clear-bottom assay plates (Costar, Tewksbury MA) at 37 °C. The reactions consisted of 10 μ L assay

buffer (50 mM HEPES, 50 mM NaCl, various pH), 10 μ L enzyme, and 30 μ L of substrate diluted in assay buffer. All enzymes were derived from homogenous purified bacterial cell extracts. For kinetic assays, each protein was examined at its optimal pH using assay buffer and 800 μ M PNPG diluted in the appropriate assay buffer. For assays at pH 6.5 to 7.4, initial 50 μ L, product formation was measured over time via absorbance at 410 nm with a PHERAstar Plus microplate reader (BMG Labtech, Ortenberg, Germany).

III. SN-38G Assay

Reactions were conducted in triplicate in 96-well, black, clear-bottom assay plates (Costar, Tewksbury MA) at 37 °C. The reactions consisted of 10 μ L assay buffer (50 mM HEPES, 50 mM NaCl, various pH), 10 μ L enzyme, and 30 μ L of SN-38G diluted in assay buffer. Processing of SN-38G was measured over time using a final concentration of 5nM enzyme and 1-50 μ M SN-38G. Formation of SN-38 was

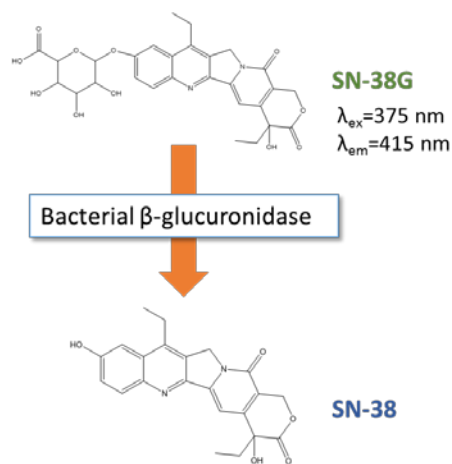


Figure 2. Schematic of the SN-38G assay

measured by excitation and emission wavelengths of 375 and 415 nm, respectively with a PHERAstar Plus microplate reader (BMG Labtech, Ortenberg, Germany).

IV. Glucuronic Acid Growth Curves

Escherichia coli strain DH5 α cultures (10 mL) were grown overnight in Luria broth in a 37° shaker. 5 mL of culture was aliquoted and 50 μ L of 100mM PNPG was added¹⁰. This was the “pulsed” group. An equivalent amount of water was added to 5 mL of “control” culture. The culture was placed back in the shaker. After 1 hour had elapsed, the culture was spun down and

resuspended in M9 minimal media without any carbon source and adjusted to an OD_{600} of 0.01. For these growth curves, D-Glucuronic acid sodium salt monohydrate (Sigma-Aldrich) was used. 1 μ L of 1000x stock glucuronic acid in water was added to the cell suspension in order to obtain the desired final concentration. The culture was plated in a 96 well, black, clear bottom, assay plate (Costar, Tewksbury MA) and the absorbance at 600nm was measured with a plate reader (Tecan) every 60-120 min.

V. RNA extraction and qPCR

RNA was extracted from 1 mL aliquots of the pulsed and control groups using the Trizol® Max™ Bacterial RNA Isolation Kit protocol. cDNA was synthesized from RNA by following the SuperScript™ Reverse Transcriptase (Invitrogen) protocol. qPCR was carried out using SYBR green as the indicator dye in a 30 μ L reaction volume.

VI. Glucuronide Growth Curves

Escherichia coli strain DH5 α cultures were grown overnight in Luria broth in a 37° shaker. 5mL of culture was aliquoted and 50 μ L of 100mM PNPG was added. The culture was placed back in the shaker. After 1 hour had elapsed, the culture was spun down and resuspended in M9 minimal media without any carbon source and adjusted to an OD_{600} of 0.1. To this, 1 μ L of 1000x stock glucuronide (E3G or DCF-G) in water was added, in order to obtain the desired final concentration. Bacteria were suspended in M9 minimal media without carbon, M9 with 100 μ M glucuronic acid and M9 with glucose as controls. The culture was plated in a 96 well, black, clear bottom, assay plate (Costar, Tewksbury MA) and the absorbance at 600nm was measured with a plate reader (Tecan) every 60 min.

Results

PNPG Processing Kinetics of *B. dorei*

The PNPG assay was run several times until consistent values of V_{\max} and K_m were obtained. 10nM of purified GUS extract and a range of 50-700 μ M PNPG was used. SigmaPlot 13.0 was used for statistical analysis.

Table 1. Table of the kinetic characteristics of *B. dorei* GUS when processing PNPG

	Value	\pmStd Error	95% Conf. Interval
V_{\max}	12 μ M/min	1 μ M/min	10 to 15 μ M
K_m	266 μ M	54 μ M	154 to 379 μ M
k_{cat}	21 s^{-1}	2 s^{-1}	
k_{cat}/K_m	0.08 $\text{s}^{-1}\mu\text{M}^{-1}$		
R^2	0.913		

Michaelis-Menten

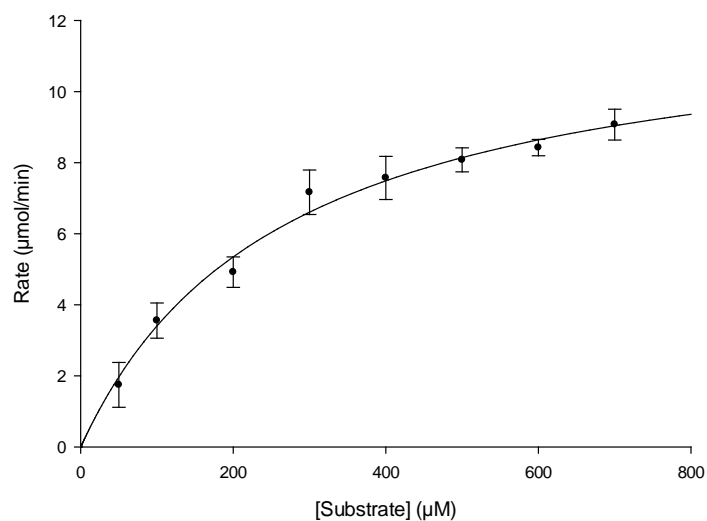


Figure 3. Michaelis-Menten curve illustrating V_{\max} and K_m of *B. dorei* GUS when processing PNPG. Error bars are standard errors of the mean.

SN-38G Processing Kinetics of *B. dorei*

The SN-38G assay was run several times until consistent values of V_{\max} and K_m were obtained. 5nM of *B. dorei* GUS was used over a range of 1-50 μ M SN-38G. SigmaPlot 13.0 was used for statistical analysis.

Table 2. Table of the kinetic characteristics of *B. dorei* GUS when processing SN-38G

	Value	\pm Std Error	95% Conf. Interval
V_{\max}	$2.9 \times 10^{-2} \mu\text{M}/\text{sec}$	$1.0 \times 10^{-3} \mu\text{M}/\text{sec}$	2.7×10^{-2} to $3.1 \times 10^{-2} \mu\text{M}$
K_m	21 μM	1.8 μM	18 to 25 μM
k_{cat}	5.9 s^{-1}	0.2 s^{-1}	
k_{cat}/K_m	$0.3 \text{ s}^{-1}\mu\text{M}^{-1}$		
R^2	0.991		

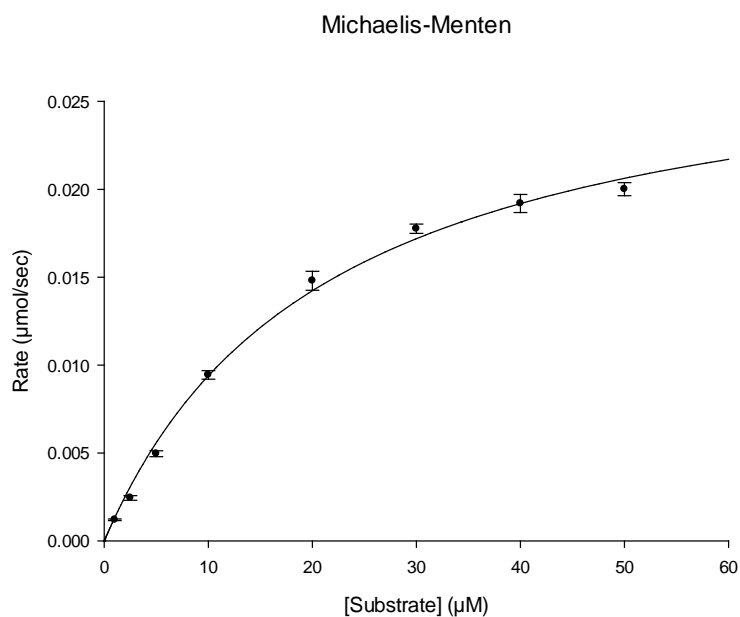


Figure 4. Michaelis-Menten curve illustrating V_{\max} and K_m of *B. dorei* GUS when processing SN-38G. Error bars are standard errors of the mean.

***E. coli* Growth in Glucuronic Acid when Pulsed vs. Control and GUS Expression Changes**

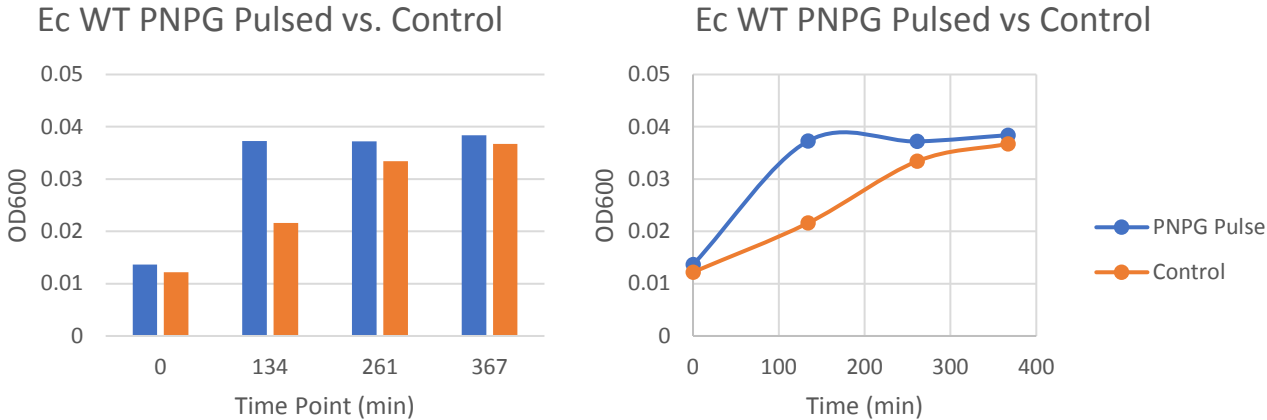


Figure 5. (A/B) Growth of *E.coli* wild type over time when pulsed

Table 3. Table of Ct values and expression fold change between pulsed and control in *E. coli*¹

dCT		ddCT	Expression fold change
Pulsed	Control	-2.3	5.1
10.8	13.2		

1. Target gene: EcGUS, Housekeeping gene: 16S rRNA

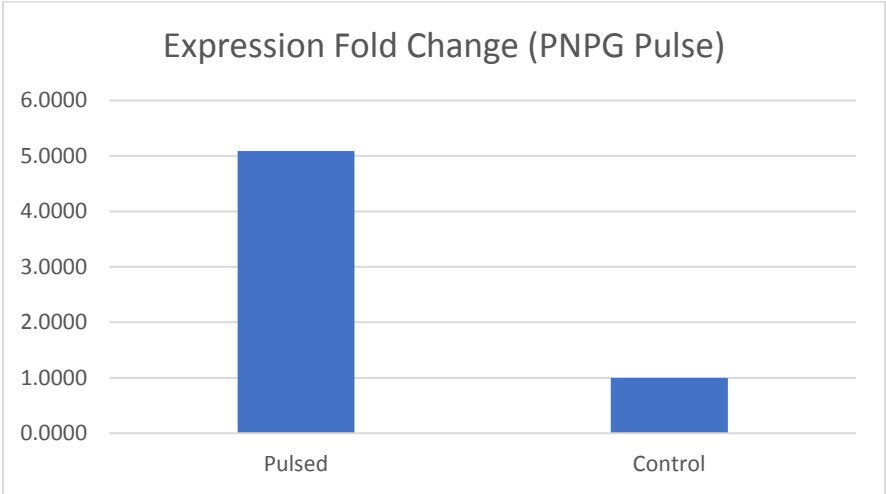


Figure 6. Pulsing with PNPB causes GUS to be 5x more expressed in *E. coli* than non-pulsed control cells.

Estriol Glucuronide (E3G) Growth Curve

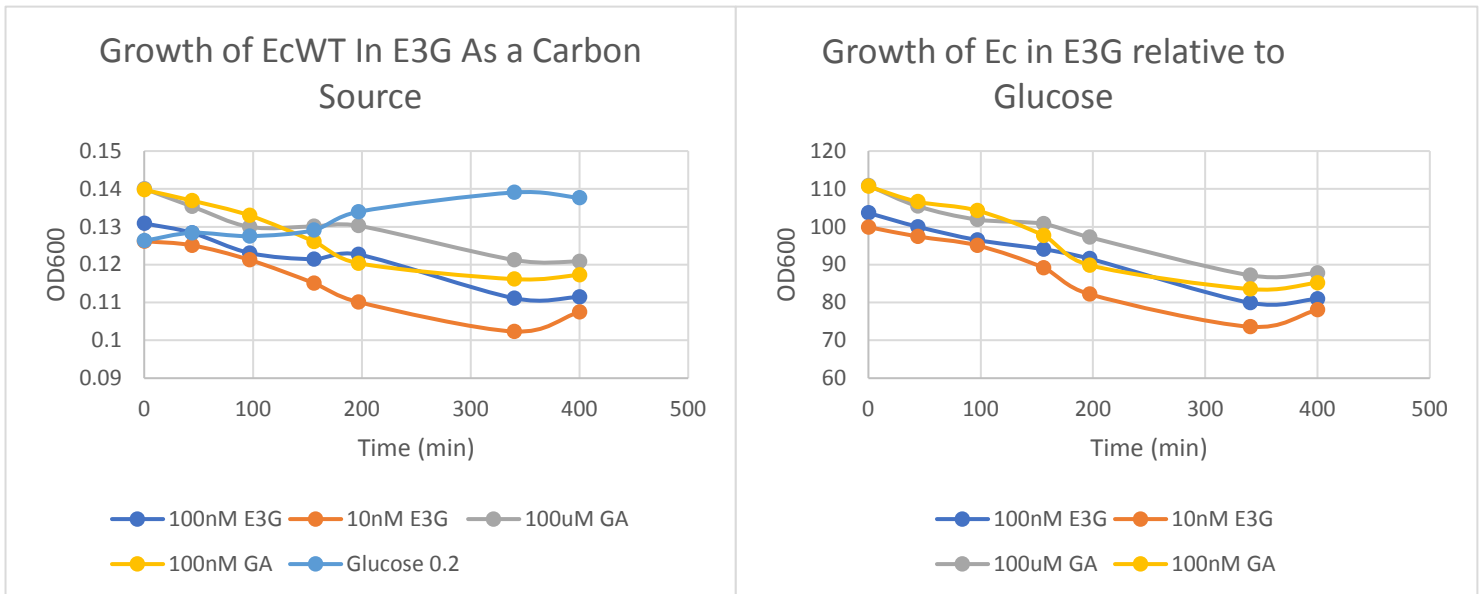


Figure 7. (A) E3G was added to M9 as the primary source of carbon and growth curves were obtained. Controls are 100 μ M GA, 100 nM GA and glucose (0.2%). (B) Representation of the data in (A) as a percent of the glucose group.

Diclofenac Glucuronide (DCF-G) Growth Curve

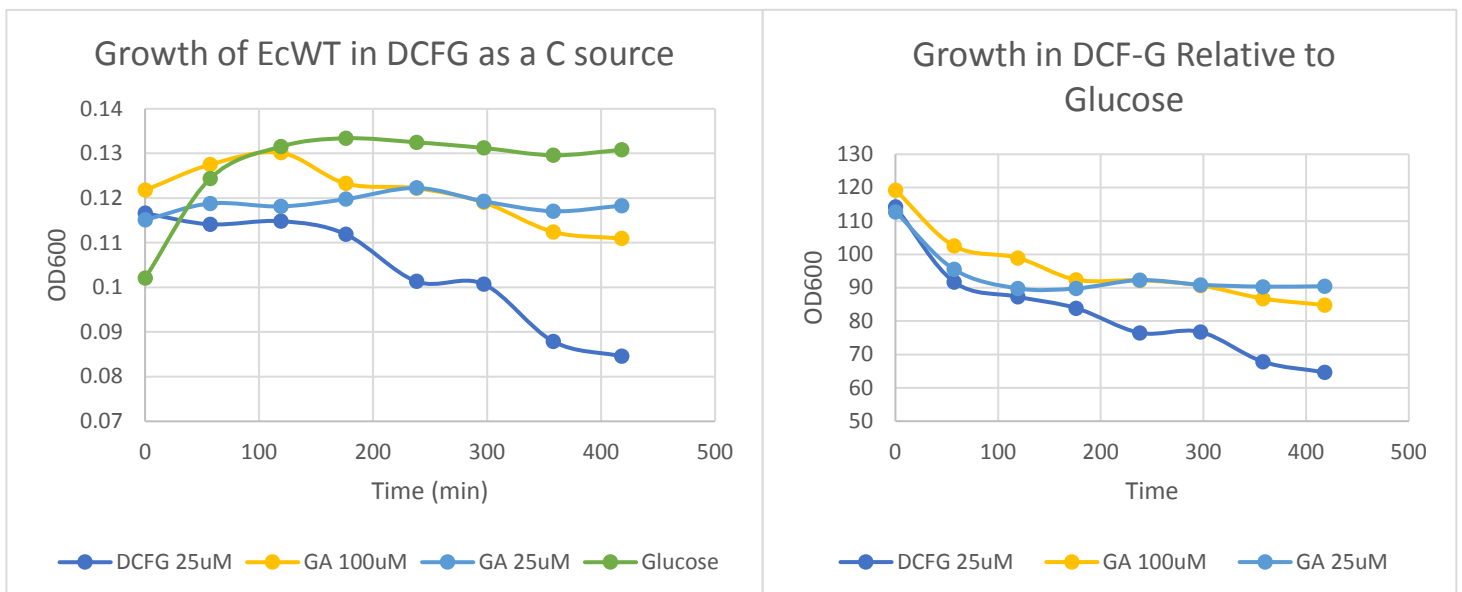


Figure 8. (A) Growth of *E. coli* WT with DCF-G as the carbon source. (B) Growth in DCF-G relative to growth in glucose.

Discussion

Part 1. Kinetic Characterization of *Bacteroides dorei*

Bacteroides dorei is a representative member of the no loop (NL) category of GUS enzymes in the human microbiota. This category makes up on average 49% of the GUS enzymes in an individual⁷. While the GUS kinetics have been studied and characterized for representative Loop 1 (L1), Loop 2 (L2) and Mini Loop 1 (mL1) species, not much is known about the characteristics of NL GUS enzymes. Because inhibitors bind to this loop region, understanding the kinetic characteristics of this large group of structurally different GUS is critical to determining the efficacy of inhibitors and chemotherapeutic treatment.

Values that characterize the kinetics of an enzyme include V_{\max} , the maximum rate at which an enzyme can process its substrate, K_M , a measure of the affinity of an enzyme for its substrate, obtained by determining the substrate concentration at half of V_{\max} , k_{cat} a first-order rate constant for the enzyme that



Figure 9. Sequence alignment of GUS from several different species. L1 species *E. coli*, *S. agalactiens* and *E.eligens*. *B. fragilis* is a representative of mL1. *B. uniformis* is a representative of L2. *B. dorei* does not have loops in either region so it is representative of NL (Pollet).

indicates how quickly the enzyme is turning over the substrate, and k_{cat}/K_M , a measure of catalytic efficiency. These values can be inexpensively measured through the PNPG assay for GUS. For *B. dorei* at 10 nM, the V_{\max} was 12.48 $\mu\text{M/s}$ (Table 1). From this, k_{cat} can be derived, and it was found to be $21 \pm 2 \text{ s}^{-1}$ which is much lower compared to the k_{cat} of *E. coli* GUS (L1) of

$120 \pm 12 \text{ s}^{-1}$, determined by members of the Redinbo Lab. However, this is higher than *B. fragilis* (mL1) which has a k_{cat} of $18 \pm 1 \text{ s}^{-1}$ and *B. uniformis*, which has a k_{cat} of 4.5 s^{-1} (Redinbo Lab). Therefore, while it doesn't have the highest rate of turnover, it is faster than some enzymes at turning over the substrate. Despite this increased rate, *B. dorei* has a low affinity for PNPG as a substrate. When run at 10 nM, the K_M was determined to be 266 μM . The low affinity for *B. dorei* for the substrate may be attributed to the lack of a loop motif around the active site. A possible function of the loop is that it could obstruct the substrate from leaving the active site, resulting in tighter binding. However, kinetic studies of *B. dorei* illustrate that this loop is not necessary to process PNPG.

While the PNPG assay gives a good estimate for the activity of GUS enzymes, testing needs to be done on actual chemotherapeutic compounds in order to obtain real-life information

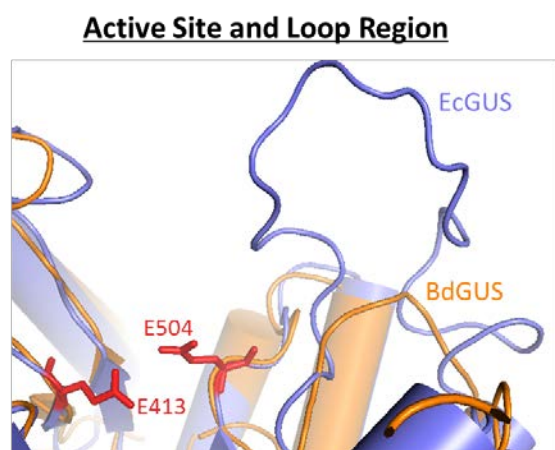


Fig 10. Active site comparison of *E. coli* (L1) and *B. dorei* (NL) active sites

on the processing activity of GUS on chemotherapeutics, such as SN-38. The SN-38G assay operates in a similar manner to the PNPG assay, where free SN-38 is measured. From this, the kinetics of *B. dorei* GUS when processing SN-38G can be determined. The V_{max} was found to be $2.9 \times 10^{-2} \pm 1.0 \times 10^{-3} \mu\text{M}/\text{sec}$ and the K_M was found to be $21 \pm 1.8 \mu\text{M}$. The k_{cat} was calculated to be $5.9 \pm 0.2 \text{ s}^{-1}$ and the catalytic efficiency (k_{cat}/K_M) was 0.3 s^{-1} . The V_{max} and k_{cat} are both lower than processing SN-38G than when *B. dorei* GUS processes PNPG, however the K_M is also lower, meaning that *B. dorei* binds SN-38G better than it does PNPG. As a result, the catalytic efficiency is $0.28 \mu\text{M}^{-1} \text{ s}^{-1}$ when cleaving SN-38G, which is much higher than a catalytic

efficiency of $0.078 \mu\text{M s}^{-1}$ when cleaving PNPG. A summary of this data is available in Table 2 and in Figure 4. In comparison to other representative enzymes, *B. dorei* processes SN-38G less effectively, however it still does to some extent. (Figure 11). Therefore, inhibitors that require a loop to bind GUS may not work because this GUS lacks a loop at the active site (Figure 10). Because the NL class of GUS is the most prevalent⁷, inhibitors that work against these enzymes are critical. In the future, experiments that test the effectiveness of inhibitors on annulling *B. dorei* GUS activity, and if needed, development of new inhibitors could greatly increase chemotherapeutic efficacy.

Part 2. Response and Growth of *E. coli* to introduction of different two different compounds.

When bacteria cleave glucuronide sugars off of different compounds, they can use it as an alternative carbon source to glucose or sucrose in the intestinal tract¹⁰. As an individual undergoes chemotherapy, they get large doses of drugs at a time. Drugs and other compounds can modulate the composition of the microbiota over time, which can cause unwanted pathogens to invade the GI tract leading to side effects and unwanted symptoms.¹¹ A key component to understanding how and why the composition of the microbiota changes is to understand how bacteria respond to different glucuronidated compounds and how their growth changes.

To mimic the introduction of drugs to the gut, cultures of *E. coli* were pulsed with PNPG for one hour, and their growth on glucuronic acid (GA) as a carbon source was monitored (Figure 5A/B). The GUS operon is not constitutively expressed; rather it needs to be induced.¹⁰ Incubating bacteria with a high concentration of glucuronidated compound can induce the GUS operon, causing cells to make a higher level of GUS protein¹⁰. It was found that *E. coli* pulsed with PNPG could grow on GA as a sole carbon source much more quickly than the control. The

lag phase of the pulsed cells is much shorter, and they enter the log phase more quickly. Pulsing these cells likely induced the GUS operon to produce GUS enzyme. Through qPCR, it was determined that the GUS expression levels increased by five-fold in the pulsed group (Figure 6). This could indicate that GUS is more highly produced by intestinal bacteria after an individual has undergone a round of chemotherapy.

The growth of bacteria on two different glucuronidated compounds: Estriol-G (E3G) and Diclofenac-G (DCF-G) was studied. Estriol is one of three main estrogen compounds produced in the body. It almost exclusively produced during pregnancy, and the glucuronidated form is excreted. The growth of *E. coli* on 10nM and 100nM concentrations of E3G as a carbon source was tested. It was found that these concentrations were not sufficient to support growth, as neither exhibited a true growth curve, and the OD readings continually decreased (Figure 7). However, there is a slight uptick in growth in the 100nM E3G group at 197 min. That could indicate the bacteria were beginning the log phase of growth, but could not fully enter the log phase due to insufficient carbon. The growth of *E. coli* on higher concentrations of E3G is a future experiment that could give insight into the growth of *E. coli* on this substrate.

In the growth curves with DCF-G as the carbon source, the trend was generally the same as the E3G group (Figure 8). The DCF-G group did not grow, and after 176 minutes, the OD readings began to decrease, indicating cell death. Despite having a higher concentration of substrate (25 μ M), the bacteria still did not grow. However, in comparison to the E3G group, which declined from the start, they did not begin decreasing until much later. This could potentially indicate that with this higher concentration of substrate, the bacteria were able to survive, but could not meet the energetic demands of reproduction. Tracking the growth of *E. coli* in higher concentrations of glucuronidated substrates is the next step in understanding how

bacteria grow in these conditions, and understanding the factors underlying fluctuations in the composition of the gut flora in patients undergoing chemotherapy.

Conclusions

In this study, the kinetic characteristics of β -glucuronidase from the bacterial species *B. dorei* when processing two substrates: PNPG and SN-38G were determined. *B.dorei* GUS is representative of the No Loop category of GUS enzymes, which are on average, the most abundant category of GUS in the human microbiota. Because existing inhibitors require the use of a loop motif near the active site, these kinetic parameters are important to understand in order to predict efficacy of inhibitors in humans. *B. dorei* GUS was overall less efficient than representatives of the other categories of GUS at processing PNPG and SN-38G, however it is crucial to note that it still retains some processing ability. This may limit the efficacy of existing inhibitors. However, this class of bacteria also provides a new useful target for inhibitor studies that can improve the efficacy of chemotherapeutics. In studying the response and growth of *E. coli* to glucuronidated compounds, it was found that pulsing bacteria with a high concentration of glucuronidated compound (in this case, PNPG), which mirrors the increase in glucuronidated compounds in the gut after a dose of chemotherapeutic, induced the GUS operon, leading to a five-fold increase in GUS production. These bacteria were then grown in either glucuronidated estriol or glucuronidated diclofenac. However, analysis of growth of bacteria in media containing either of these compounds remains inconclusive. Further studies using higher concentrations can determine the growth dynamics of bacteria on several common glucuronidated compounds. Combined with studies of enzyme kinetics, this can give insight into the compositional changes of the gut flora in patients being treated with chemotherapeutic drugs and help improve targeted, personalized therapy for patients in the future.

References

1. Gagnière, J. et al. Gut microbiota imbalance and colorectal cancer. *World Journal of Gastroenterology*, **2016**, 22:2, 501-518.
2. Wallace, B.D et al. Structure and Inhibition of Microbiome β -Glucuronidases Essential to the Alleviation of Cancer Drug Toxicity. *Chemistry & Biology* **2015**, 22, 1238–1249.
3. B. D. Wallace et al., *Science* **2010** 330, 831.
4. I. Husain, J. L. Mohler, H. F. Seigler, J. M. Besterman, *Cancer Res.* 54, 539 (1994).
5. Gupta, E. et al. Metabolic Fate of Irinotecan in Humans: Correlation of Glucuronidation with Diarrhea. *Cancer Research*, **1994**, 2, 3723-3725.
6. Wallace, B.D. et al. Alleviating Cancer Drug Toxicity by Inhibiting a Bacterial Enzyme. *Science* **2010**, 330, 831-835.
7. Pollet, R.M. et al. An Atlas of β -glucuronidases in the Human Intestinal Microbiome. *Structure*. In press.
8. Saitta, K.S. et al. Bacterial β -glucuronidase inhibition protects mice against enteropathy induced by indomethacin, ketoprofen or diclofenac: mode of action and pharmacokinetics. *Xenobiotica*, **2014**. 44:1 28-35.
9. Sarda S, Page C, Pickup K, et al. Diclofenac metabolism in the mouse: novel in vivo metabolites identified by high performance liquid chromatography coupled to linear ion trap mass spectrometry. *Xenobiotica* **2012** 42:179–94.
10. Wilson, K.J. et al. “The Escherichia coli gus Operon: Induction and Expression of the gus Operon in E. coli and the Occurrence and Use of GUS in Other Bacteria” *GUS Protocols: Using the GUS Gene as a Reporter of Gene Expression*. Academic Press Inc. **1992**.

11. Redinbo, M.R. The Microbiota, Chemical Symbiosis, and Human Disease. *J. Mol. Biol.* **2014**, 426:23, 3877-3891.